Electronic Supplementary Material (ESI) for Journal of Materials Chemistry A.

Supplementary Information

Solvent- and catalyst-free mechanochemical synthesis of alkali metal hydrides

Ihor Hlova,[a,c] Andra Castle,[a,b] Jennifer F. Goldston,[a,b] Shalabh Gupta,*[a] Tim Prost,[a,c] Takeshi Kobayashi,[a] L. Scott Chumbley,[a,c] Marek Pruski[a,b] and Vitalij K. Pecharsky[a,c]

[a.] *Ames Laboratory, Iowa State University, Ames, IA 500011-3020, USA. Email address: Shalabh@ameslab.gov*
[b.] *Department of Chemistry, Iowa State University, Ames, IA 500011-3111, USA.*
[c.] *Department of Materials Science and Engineering, Iowa State University, Ames, IA 50011-2300, USA.*

S.1.1 Estimated quadrupolar coupling constants C_Q (for $\eta = 0$)

Table S1. ^{7}Li quadrupolar parameters as obtained via Dmfit[1]. The η_Q is the quadrupolar asymmetry parameter and ν_Q and C_Q are the quadrupolar coupling constant where $\nu_Q = 3\ C_q / 2I(2I-1)$. I=3/2 for ^{7}Li

Sample	ν_Q (kHz)[a]	C_Q (kHz)[a]	η_Q[b]
com-LiH	26.90	53.8	0.00
com-LiD	24.87	49.74	0.00
as-LiH-2	29.11	58.22	0.00
as-LiH-4	27.67	55.34	0.00
as-LiH-8	25.89	51.78	0.00
as-LiH-12	26.49	52.98	0.00
as-LiH-20	26.53	53.06	0.00
as-LiH-40	26.86	53.72	0.00
avg[c]	27.09	54.18	0.00
sdev[c]	1.15	2.29	0.00

[a] Where each sample was fitted independently.

[b] $\eta_Q = 0$ was assumed for all samples since the asymmetry cannot be accurately assessed from MAS spectra in the case of such weak quadrupolar coupling.

[c] Based on the as-synthesized LiH samples, only.

S.1.2 Determination of Spin Lattice Relaxation Times T_1 via Saturation Recovery

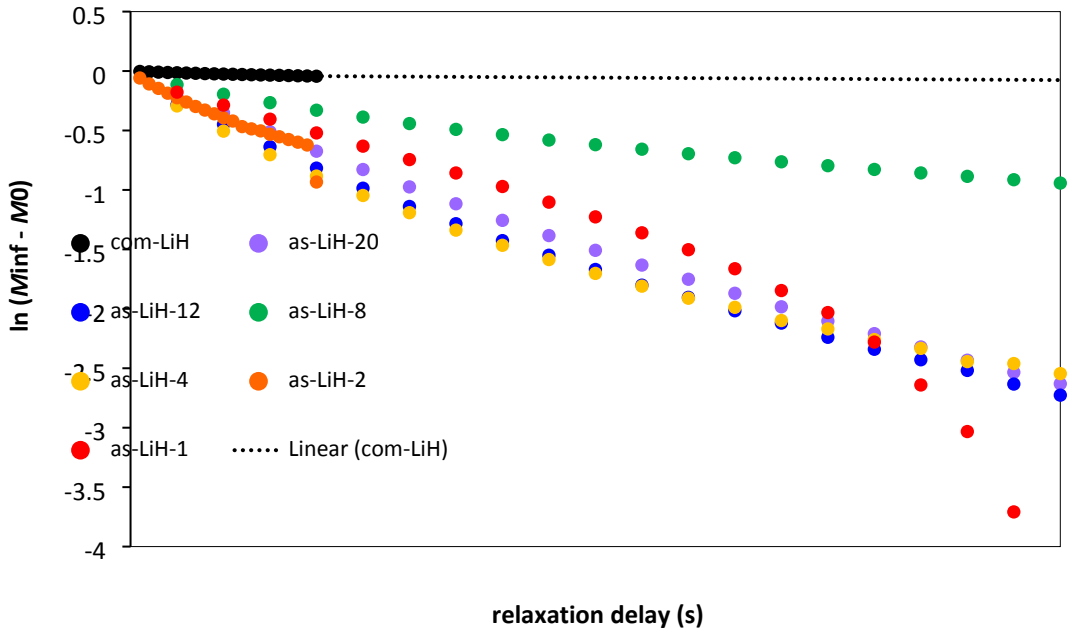

Figure S1. Semi-log plot of the saturation recovery curves obtained from samples milled for various times between 1 and 20 h (as-LiH-1 to as-LiH-20).

Table S2. T_1 relaxation times for *as*-synthesized (as-LiH-1 to as-LiH-20) materials and commercial LiH as obtained by least-squares fitting of the saturation recovery with a single-exponential function.

Sample	T_1 (s)	R^2
as -LiH-1	30	0.9282
as -LiH-2	29	0.9325
as -LiH-3	27	0.9539
as -LiH-4	44	0.9724
as -LiH-6	29	0.9274
as -LiH-8	120	0.9768
as -LiH-12	40	0.9879
as -LiH-20	40	0.9952
com -LiH	2500	0.9834

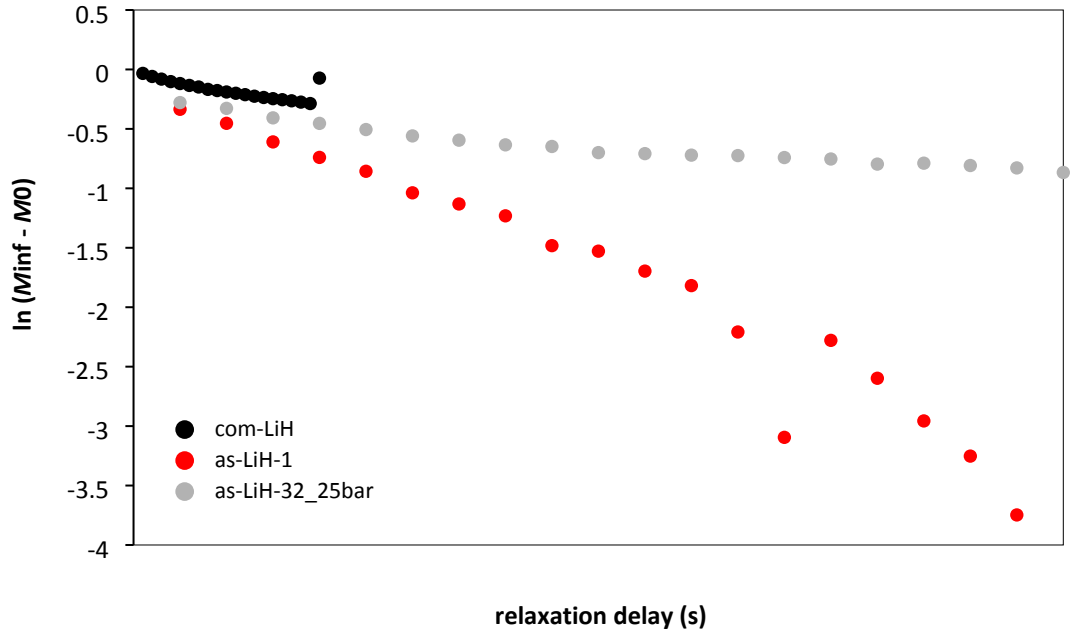

Figure S2. Semi-log plot of the saturation recovery curves for metallic lithium obtained using the materials indicated in the plot legend.

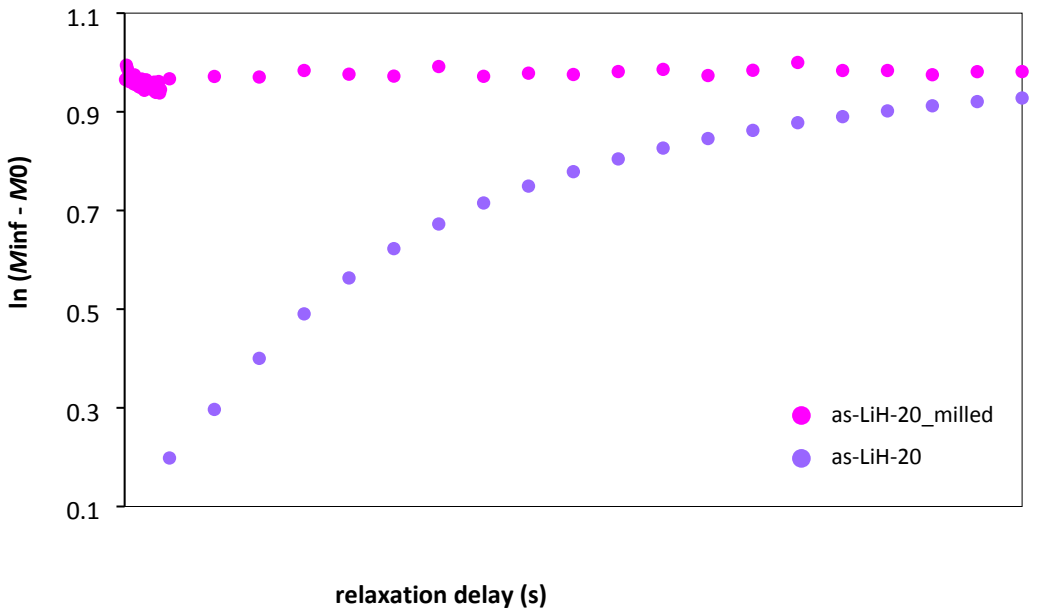

Figure S3. Comparison of *as*-synthesized LiH (as-LiH-20) with *as*-LiH-20 milled (milled for additional 20 h post synthesis in an inert Ar atmosphere). T_1 of *as*-LiH-20_milled is << 1 s.

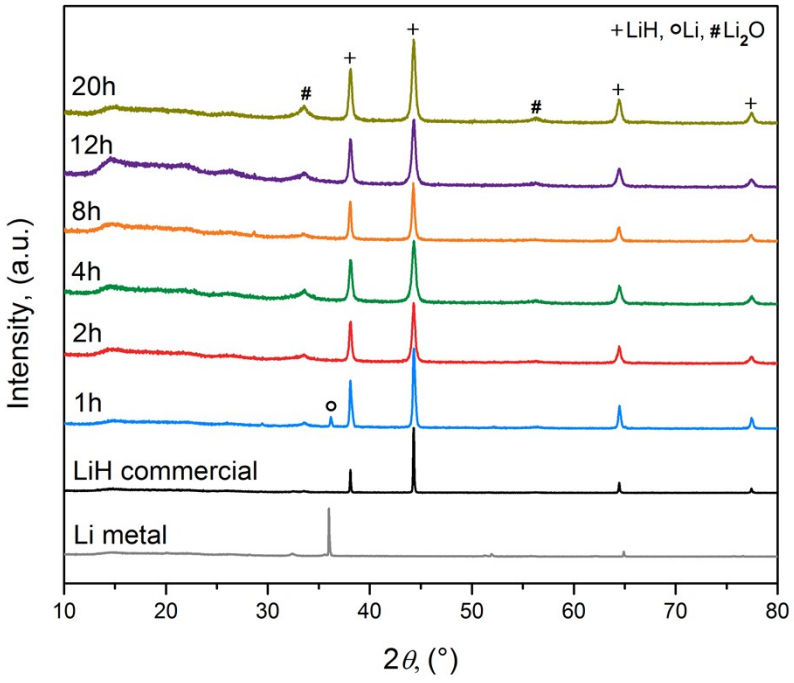

Figure S4. X-ray diffraction patterns shown as scattered intensity vs. Bragg angle (and as contour plots in Fig. 1(a)) obtained from the samples produced in a magnetic ball mill as a function of milling duration.

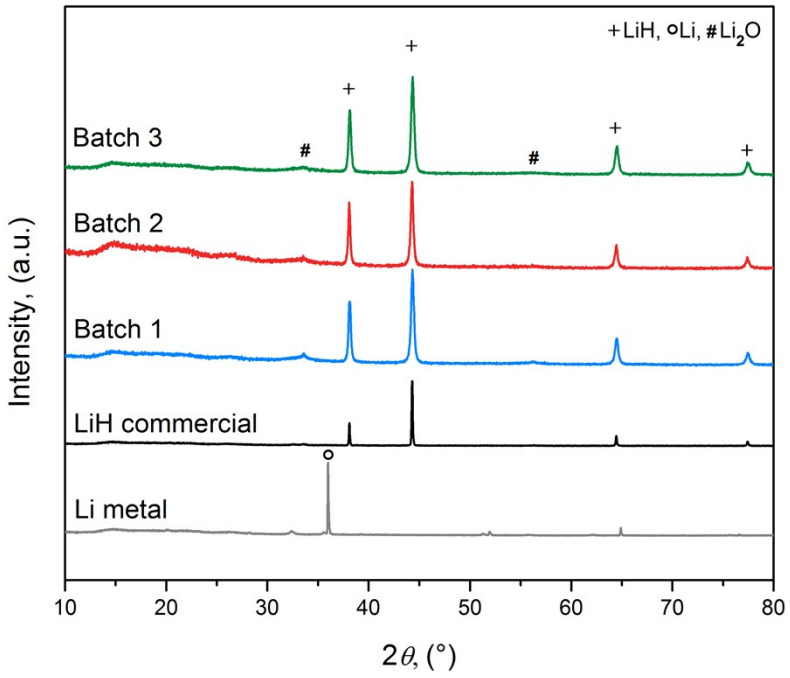

Figure S5. X-ray diffraction patterns shown as scattered intensity vs. Bragg angle (and as contour plots in Fig. 5) for LiH obtained after three consecutive milling each of 16 hour duration.

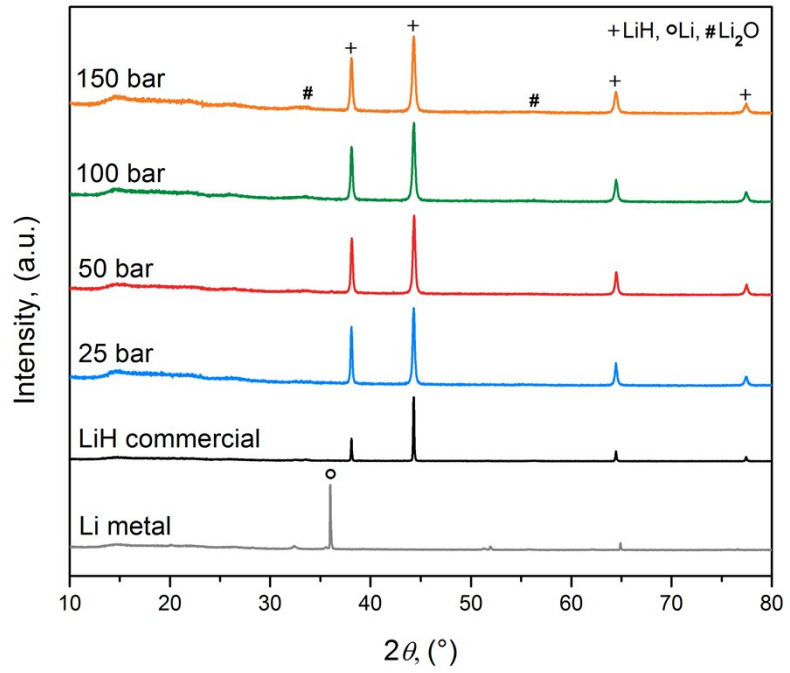

Figure S6. X-ray diffraction patterns shown as scattered intensity vs. Bragg angle (and as contour plots in Fig. 6) of LiH powder obtained from milling 1:1 mixture (by wt.) of Li metal and pre-formed LiH powder in a planetary ball mill for 1 h under varying hydrogen pressure.

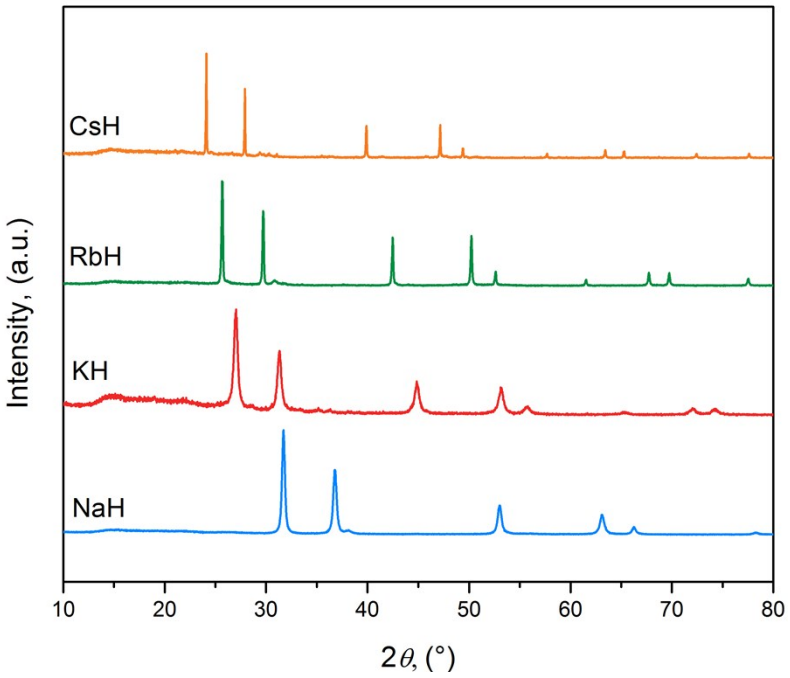

Figure S7. X-ray diffraction patterns shown as scattered intensity vs. Bragg angle (and as contour plots in Fig. 7) of *as*-synthesized NaH, KH, RbH, and CsH as described in sections 3.2–3.4.

References

[1] Massiot *et al., Magn. Reson. Chem.* **2002**, 40, 70-76.